Redox Biology 75 (2024) 103255

Contents lists available at ScienceDirect

Redox Biology

journal homepage: www.elsevier.com/locate/redox

Inhibition of ferroptosis rescues M2 macrophages and alleviates arthritis by suppressing the HMGB1/TLR4/STAT3 axis in M1 macrophages

Zhuan Feng [a,b,1], Feiyang Meng [a,b,1], Fei Huo [a,b,1], Yumeng Zhu [a,b], Yifei Qin [a,b], Yu Gui [a,b], Hai Zhang [a,b], Peng Lin [a,b], Qian He [a,b], Yong Li [c,***], Jiejie Geng [a,b,**], Jiao Wu [a,b,*]

[a] Department of Cell Biology of National Translational Science Center for Molecular Medicine and Department of Clinical Immunology of Xijing Hospital, Fourth Military Medical University, Xi'an, 710032, Shaanxi, China
[b] State Key Laboratory of New Targets Discovery and Drug Development for Major Diseases, China
[c] National-Local Joint Engineering Research Center of Biodiagnostic & Biotherapy, The Second Affiliated Hospital, Xi'an Jiaotong University, Xi'an, Shaanxi, 710004, China

ARTICLE INFO

Keywords:
Rheumatoid arthritis
Ferroptosis
Macrophage

ABSTRACT

Ferroptosis is a type of programmed cell death driven by iron-dependent lipid peroxidation. The TNF-mediated biosynthesis of glutathione has been shown to protect synovial fibroblasts from ferroptosis in the hyperplastic synovium. Ferroptosis induction provides a novel therapeutic approach for rheumatoid arthritis (RA) by reducing the population of synovial fibroblasts. The beginning and maintenance of synovitis in RA are significantly influenced by macrophages, as they generate cytokines that promote inflammation and contribute to the destruction of cartilage and bone. However, the vulnerability of macrophages to ferroptosis in RA remains unclear. In this study, we found that M2 macrophages are more vulnerable to ferroptosis than M1 macrophages in the environment of the arthritis synovium with a high level of iron, leading to an imbalance in the M1/M2 ratio. During ferroptosis, HMGB1 released by M2 macrophages interacts with TLR4 on M1 macrophages, which in turn triggers the activation of STAT3 signaling in M1 macrophages and contributes to the inflammatory response. Knockdown of TLR4 decreased the level of cytokines induced by HMGB1 in M1 macrophages. The ferroptosis inhibitor liproxstatin-1 (Lip-1) started at the presymptomatic stage in collagen-induced arthritis (CIA) model mice, and GPX4 overexpression in M2 macrophages at the onset of collagen antibody-induced arthritis (CAIA) protected M2 macrophages from ferroptotic cell death and significantly prevented the development of joint inflammation and destruction. Thus, our study demonstrated that M2 macrophages are vulnerable to ferroptosis in the microenvironment of the hyperplastic synovium and revealed that the HMGB1/TLR4/STAT3 axis is critical for the ability of ferroptotic M2 macrophages to contribute to the exacerbation of synovial inflammation in RA. Our findings provide novel insight into the progression and treatment of RA.

1. Introduction

Rheumatoid arthritis (RA) is a chronic systemic autoimmune disease characterized by persistent articular inflammation and joint damage caused by synovial fibroblasts as well as a dysregulated immune response [1]. Emerging evidence has demonstrated that the innate immune system is essential for the onset and development of RA pathogenesis. In addition to causing inflammatory reactions, a variety of innate immune cells, including monocytes, macrophages, and dendritic cells, are also responsible for initiating the activation of the adaptive immune system, which is crucial in the advanced phases of the disease. The infiltration of synovial macrophages is associated with the pathogenesis of RA. One key feature of macrophages is their plasticity, since they are able to exhibit heterogeneous phenotypes and form distinct

* Corresponding author. Department of Cell Biology of National Translational Science Center for Molecular Medicine and Department of Clinical Immunology of Xijing Hospital, Fourth Military Medical University, Xi'an, 710032, Shaanxi, China.
** Corresponding author. Department of Cell Biology of National Translational Science Center for Molecular Medicine and Department of Clinical Immunology of Xijing Hospital, Fourth Military Medical University, Xi'an, 710032, Shaanxi, China.
*** Corresponding author.
E-mail addresses: liyong0110@hotmail.com (Y. Li), gengjie-jie@163.com (J. Geng), jiaowubio@hotmail.com (J. Wu).
[1] These authors contributed equally to this work.

https://doi.org/10.1016/j.redox.2024.103255
Received 7 May 2024; Received in revised form 19 June 2024; Accepted 23 June 2024
Available online 24 June 2024

subpopulations. Depending on whether macrophages are M1-or M2-type macrophages, these cells are implicated not only in the spread of inflammation but also in its resolution. M1 macrophages are characterized by high expression of major histocompatibility complex (MHC) class II, CD80, CD86 and TLR4 and the secretion of proinflammatory cytokines, including IL-1β, IL-6 and TNF-α [2,3]. The expression of surface markers such as mannose receptor-1 (CD206), macrophage scavenger receptors (CD163 and CD204), and the MER proto-oncogene tyrosine kinase (MerTK) characterizes the anti-inflammatory M2 macrophages [4]. In both peripheral blood and synovial tissue, M1 macrophages mediate and maintain the inflammatory process in RA. An increase in the proportion of M2 macrophages through the MerTK signaling pathway effectively alleviated the progression of RA in a clinical setting [5]. Thus, the responses mediated by distinct macrophage phenotypes need to be precisely regulated to reduce inflammation and synovial tissue destruction. Remarkably, one of the early indicators of RA is the elevated level of activated proinflammatory macrophages in synovial tissue, which is associated with a greater proportion of M1 macrophages than M2 macrophages [6]. In the RA synovium, M1 macrophages are activated and interact with Th1 cells to increase the production of proinflammatory cytokines [4,7]. M2 macrophages play an anti-inflammatory role, modulating immune cell activation to promote tissue repair through IL-10 and TGF-β secretion [8,9]. There is macrophage subset disequilibrium in the synovial fluid of RA patients, with M1/M2 ratios being greater in RA patients than in OA patients [10–12].

Ferroptosis is a new type of programmed cell death related to iron-dependent lipid peroxidation. The accumulation of lipid peroxides and oxidative stress are key contributors to persistent joint inflammation [13,14]. In our previous study, we also discovered that synovial fibroblasts from RA patients exhibit increased iron accumulation and lipid peroxides [15]. Although it is believed that altering the oxidative microenvironment could be an effective strategy for increasing the efficacy of RA treatment, when the lipid peroxidation inhibitor liproxstatin-1 (Lip-1) was used after the onset of notable arthritic symptoms, it was unable to prevent the progression of inflammation and joint damage. On the other hand, the administration of lipid peroxidation inhibitors beginning in the presymptomatic phases of arthritis effectively prevented the onset of joint inflammation [15]. However, the interactions between synovial macrophages and ferroptosis in mediating the joint inflammatory process during RA are largely unexplored.

In this study, we established a widely used collagen-induced arthritis (CIA) mouse model and a collagen antibody-induced arthritis (CAIA) mouse model to elucidate the effect of ferroptosis on the macrophage population in the pathogenesis of RA. In RA patients, CIA model mice, and CAIA model mice, the hyperplastic rheumatoid synovium was enriched in macrophages compared with that in OA patients or normal mice. Single-cell RNA sequencing of cells from the hyperplastic synovium of RA patients revealed that ferroptosis-related pathways were enriched in M2 macrophages. Compared with M1 macrophages, M2 macrophages were more sensitive to ferroptosis induction. HMGB1 released by ferroptotic M2 macrophages interacted with Toll-like receptor 4 (TLR4) expressed on M1 macrophages and exacerbated inflammatory cytokine secretion during CIA or CAIA progression by activating the STAT3 signaling pathway. Additionally, pretreatment with GPX4-overexpressing M2 macrophages or the ferroptosis inhibitor Lip-1 significantly ameliorated joint inflammation and destruction by inhibiting ferroptosis in M2 macrophages, resulting in anti-inflammatory effects, particularly against inflammation induced by M1 macrophages, in the CIA and CAIA mouse models. In conclusion, our findings demonstrate that the HMGB1/TLR4/STAT3 axis driven by ferroptotic M2 macrophages increases the proportion of inflammatory M1 macrophages during the development of RA. An inhibitor of ferroptosis effectively rescues M2 macrophages and prevents the development of joint inflammation and joint destruction.

2. Results

2.1. The enrichment of macrophages in the hyperplastic synovium of RA patients, CIA model mice and CAIA model mice

We established a CIA mouse model, which is one of the most common used models of RA, via two steps of immunization and examined joint inflammation every two days for 14 days after the first immunization (Fig. 1A). Four out of ten mice that received incomplete Freund's adjuvant (IFA) vaccination developed arthritis, which was characterized by noticeably swollen toes and limited mobility. CIA model mice exhibited significant joint swelling and inflammation, as well as increased cartilage destruction and bone erosion (Fig. 1B–E). Previous studies have shown that the differentiation and function of osteoclasts, which play a critical role in bone degradation, are mainly regulated by two key cytokines, macrophage colony-stimulating factor (M-CSF) and receptor activator of NF-κB ligand (RANKL) [16]. Compared with those of control mice, the synovial tissues of hyperplastic CIA model mice appeared to contain greater levels of RANKL and M-CSF (Fig. 1F to G). These findings verified that the hyperplastic synovium in CIA model mice exhibited increased osteoclastogenesis. Multiplex immunohistochemistry (mIHC) staining revealed that $CD68^{+}$ or $F4/80^{+}$ macrophages were enriched in the hyperplastic synovium of RA patients and collagen antibody-induced arthritis mice (Figs. S1A–C) compared with those of OA patients and control mice (Fig. 1H to I).

2.2. Single-cell RNA sequencing detects synovial macrophages with distinct functions in RA patients

RA synovial macrophages from the circulation in the joint cavity can differentiate into osteoclasts to promote joint inflammation [17,18]. M1 macrophages strongly express proinflammatory cytokines, including IL-1β, IL-6 and TNF-α, which initiate the upregulation of destruction mediators in primary tissue and promote osteoclast differentiation to cause bone resorption [19–21]. To investigate the different functions of macrophages in the synovium of patients with arthritis, we analyzed single-cell RNA sequencing data from the hyperplastic synovium of 5 patients with RA. We cataloged cells into 10 distinct lineages annotated using the expression levels of canonical marker genes (Fig. 2A).

One of the most significantly enriched pathways in the macrophage subpopulation was the ferroptosis pathway. Two major polarization states have been described for macrophages: classically activated type 1 (M1) and alternatively activated type 2 (M2) (Fig. 2B). Macrophages are classically activated in vitro using bacterial cell wall components (such as LPS) and IFN-γ or TNF-α. M1 macrophages are characterized by the production of proinflammatory cytokines such as TNF-α, IL-1β, IL-6 and IL-12. M2 macrophage polarization can be induced in vitro by IL-4 and/or IL-13, TLRs, IL-1 receptor ligands or IL-10. M2 macrophages secrete anti-inflammatory cytokines such as IL-10, CCL18, and CCL22. M2 macrophages are characterized by the expression of MRC1, CD163, Dectin-1 and DC-SIGN. Some of the clusters were enriched in M1 macrophages ($CD16^{high}CD64^{high}CD163^{low}MRC1^{low}$), while some expressed markers for M2 macrophages ($CD16^{low}CD64^{low}CD163^{high}MRC1^{high}$). Pathway analysis revealed that the ferroptosis pathway was enriched in the M2 clusters (Fig. 2C). The M2 clusters also exhibited high expression of genes involved in oxidative phosphorylation, fatty acid biosynthesis and cytokine–cytokine receptor interactions. Gene expression network analysis further revealed that the genes encoding transferrin receptor 1 (TFRC) and acyl-CoA synthetase long chain family member 4 (ACSL4), both crucial mediators of ferroptosis, were upregulated in M2 macrophages (Fig. 2D to E). The accumulation of lipid peroxides and iron overload in the hyperplastic rheumatoid synovium and synovial fluid of RA patients have been confirmed [15]. Next, we used IHC to confirm the heterogeneity and changes in M1 macrophages and M2 macrophages in synovial tissue during the development of arthritis (Fig. 2F). The population of M1 macrophages (CD16) was increased in the hyperplastic

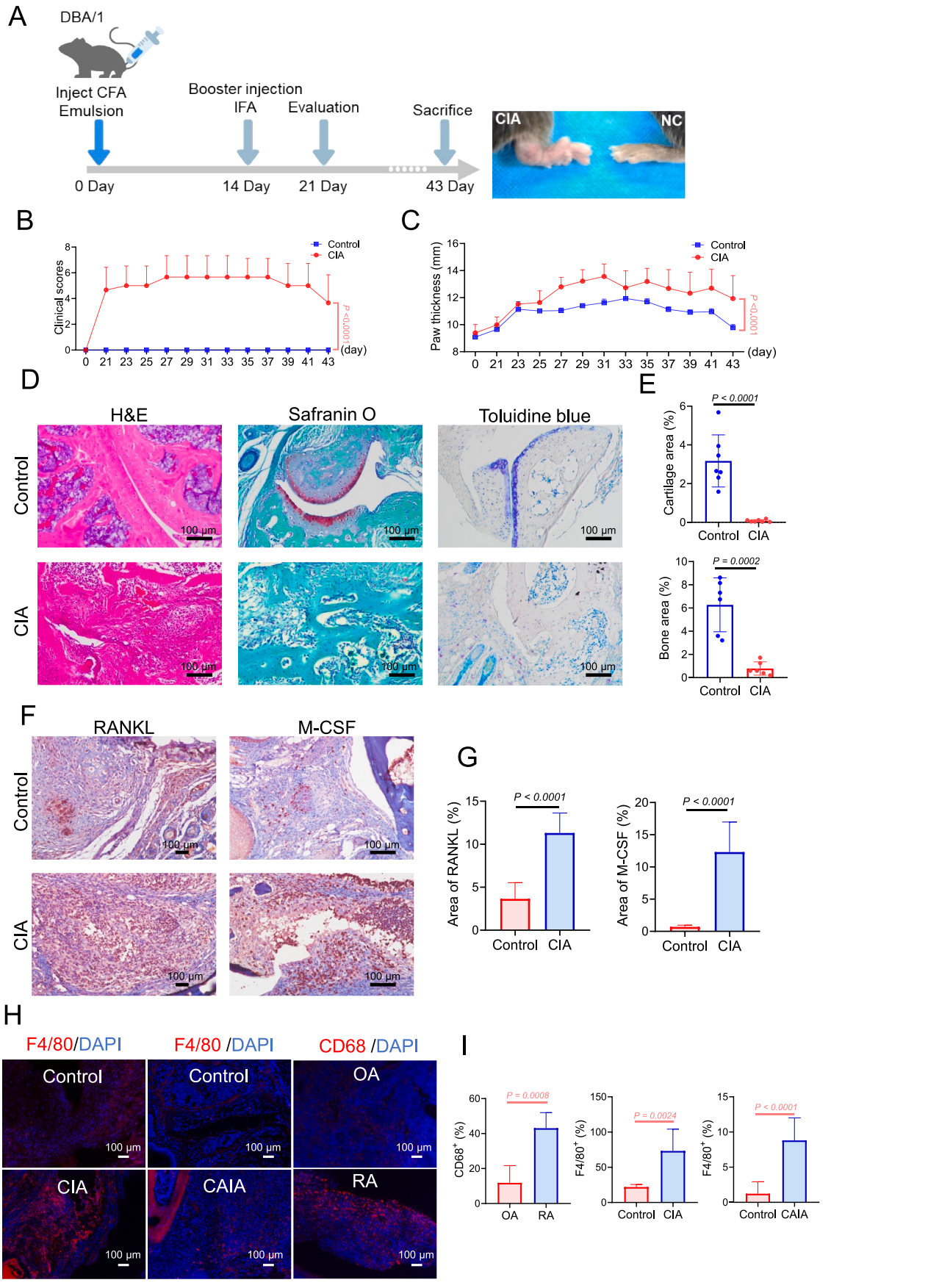

(caption on next page)

Fig. 1. The enrichment of macrophages in the synovium of RA patients and arthritis mice. **(A)** Schematic diagram for the establishment of a CIA mice model. Joint inflammation was measured by arthritis score (**B**) and paw thickness (**C**) in CIA mice, n = 3 mice for both control and CIA group. **D** Images of hematoxylin and eosin (H&E), toluidine blue, and safranin O staining of representative joints from control and CIA mice. Scale bars, 100 μm. **E** Quantification of the histomorphometric analysis of cartilage damage and bone erosion. **F** Representative immunohistochemical staining of RANKL and M-CSF in the inflamed joint tissue of CIA model mice. **G** Quantitative comparison of RANKL and M-CSF between normal and CIA model mice, with n = 6 joints for the control group and n = 9 mice for the CIA group. **H** mIHC staining of macrophage markers (human: CD68; mice: F4/80) in the synovium. Scale bars, 100 μm. **I** Quantification of the percentages of macrophage markers in hyperplastic synovium. Data are presented as mean ± SD. (For interpretation of the references to colour in this figure legend, the reader is referred to the Web version of this article.)

synovium of CIA model mice (Fig. 2G), and an imbalance in the M1/M2 ratio is the sole important factor that contributes to the number of osteoclasts, which is consistent with previous reports in the literature on RA patients [11]. Based on these results, we hypothesize that ferroptotic cell death may lead to a decrease in M2 macrophages in the rheumatic synovium.

2.3. M2 macrophages are more vulnerable to ferroptosis than M1 macrophages

To investigate the susceptibility of M1 macrophages and M2 macrophages to ferroptosis induction, we differentiated THP-1 monocyte-like cells into M0 macrophages and further polarized the cells into M1 and M2 phenotypes (Fig. 3A and Fig. S2). Once differentiated (M0 macrophages), they were incubated with IL-4 and IL-13 to obtain M2-polarized macrophages or with IFN-γ and LPS for classical macrophage activation (M1). CD206 was used to characterize the M2 phenotype, while CD86 was used to characterize the M1 phenotype (Fig. 3B and Fig. S2). The sensor in the lipid peroxidation kit changes its fluorescence from PE to FITC upon peroxidation by lipid ROS in cells, thus enabling ratio metric measurements of lipid peroxidation (a decreasing PE/FITC ratio indicates increasing lipid peroxidation). The GPX4 inhibitor RSL-3 triggered more prominent cell death, associated lipid peroxidation, and decreased cell viability in M2 macrophages than in M1 macrophages, and these effects were abolished by ferrostatin-1 (Fer-1), an inhibitor of ferroptosis (Fig. 3C–E). Moreover, compared with M1 macrophages, M2 macrophages showed increased intracellular ROS generation and ferrous iron levels induced by RSL-3 (Figs. S3A–B). The expression level of GPX4 decreased significantly in M2 macrophages treated with RSL-3 for 5 h but was inhibited by Fer-1 (Fig. 3F to G). RSL-3 also increased the expression of TFRC and the ferroptosis marker PTGS2 in M2 macrophages treated with RSL-3 for 7 h (Fig. 3H to I). This finding is consistent with the results of the single-cell sequencing of RA patients (Fig. 2D). Endogenous danger signals called damage-associated molecular pattern molecules (DAMPs) influence the inflammatory response to cell death and activate the immune system. High-mobility group box 1 protein (HMGB1) is a proinflammatory DAMP released by ferroptotic cells. ELISA analysis revealed that the release of HMGB1 from M2 macrophages increased in response to RSL-3, and this effect was blocked by Fer-1 (Fig. 3J).

2.4. HMGB1 released by ferroptotic M2 macrophages promotes the secretion of inflammatory cytokines by M1 macrophages via activation of the STAT3 pathway

For extended periods of time, HMGB1, a highly conserved ubiquitous protein, has been identified as a nuclear DNA-binding protein that is involved in nucleosome stabilization and gene transcription. HMGB1 released from activated M2 macrophages could function as an important mediator in the pathogenesis of infection and sterile inflammation. HMGB1 has been reported to be an essential factor in RA pathogenesis because of its ability to promote macrophage activation and increase the production of proinflammatory mediators [22–24]. In particular, HMGB1 is expressed in abundance in the intra-articular fluid of RA patients, primarily because of its increased concentration in patients with RA [24,25]. To explore the interaction between M1 macrophages and ferroptotic M2 macrophages in RA, we constructed an indirect coculture system (Fig. 4A). Compared with control cells, M1 macrophages cultured with the supernatant of M2 macrophages treated with RSL-3 exhibited increased levels of phosphorylated STAT3 at serine 727, and the level of phosphorylated STAT3 at tyrosine 705 did not significantly differ (Fig. 4B). The phosphorylation level of STAT3 at serine 727, IL-1β, and IL-6 were unchanged in M1 macrophages induced by RSL-3 in the presence or absence of Fer-1, excluding the possibility that residual RSL-3 in M2 supernatant may influence the related pathways in M1 macrophages (Fig. S3C). M1 macrophage DAMPs can be detected by receptors that identify patterns, such as TLRs, NOD-like receptors (NLRs), and RIG-like receptors, resulting in the activation of immune cells. Compared with angiogenesis and bone destruction, the activation of TLRs in synovial macrophages leads to the aggravation of arthritis. In the RA synovium, TLR2 and TLR4 are involved in regulating the synthesis of inflammatory components. In fact, in monocyte-derived macrophages and synovial macrophages isolated from RA patients, TLR4 activation promotes the proinflammatory activity of M1 macrophages through the synthesis and release of IL-6, TNF-α, and IL-1β [26]. The expression of TLR4 was significantly upregulated in M1 macrophages cultured with the supernatant of M2 macrophages treated with RSL-3, while the expression of TLR2 remained unchanged (Fig. 4C). In the presence or absence of an HMGB1 neutralizing antibody or the TLR4-specific signaling inhibitor TAK-242, phospho-STAT3 induced by the supernatant of RSL-3-treated M2 macrophages was markedly downregulated, suggesting that HMGB1 and TLR4 contribute to the activation of STAT3 signaling (Fig. 4D). To determine whether activated STAT3 signaling contributes to the proinflammatory production of M1 macrophages, we evaluated several classic inflammatory cytokines. We found that the expression levels of IL-1β, IL-6, and IL-17A were increased following treatment with the supernatant of ferroptotic M2 macrophages (Fig. 4E to F). In addition, a significant increase in the mRNA levels of inflammatory cytokines (Fig. 4G). Knockdown of TLR4 in M1 macrophages treated with the supernatant of ferroptotic M2 macrophages markedly decreased the expression of IL-1β, and the administration of HMGB1 increased the expression of IL-1β, which was attenuated by TLR4 knockdown (Fig. 4H–J). These findings suggest that HMGB1 released by ferroptotic M2 macrophages triggers TLR4-STAT3 signaling in M1 macrophages and contributes to the inflammatory response.

2.5. Pretreatment with the ferroptosis inhibitor Lip-1 or treatment with GPX4 overexpression vectors (AAV-DIO-Gpx4) significantly increases the proportion of M2 macrophages and reduces joint inflammation and destruction in arthritis models

To further determine the role of M2 macrophage ferroptosis in the development of arthritis, we treated mice with Lip-1 (10 mg/kg every 2 days) to inhibit ferroptosis in the CIA experimental arthritis model (start from Day 7 after the first immunization) (Fig. S4). PBMCs and spleen cells were isolated from CIA model mice with or without Lip-1 administration and stained with a lipid peroxidation sensor (the increasing PE/FITC ratio indicates decreasing lipid peroxidation) by flow cytometry. We found that cells from Lip-1-treated mice showed lower levels of lipid peroxidation (Fig. 5A to B). Moreover, Lip-1 treatment started at the presymptomatic stage of CIA and prevented the development of joint inflammation and joint destruction (Fig. 5C and E). To test whether overexpression of GPX4 can rescue M2 macrophages in arthritic mice, an

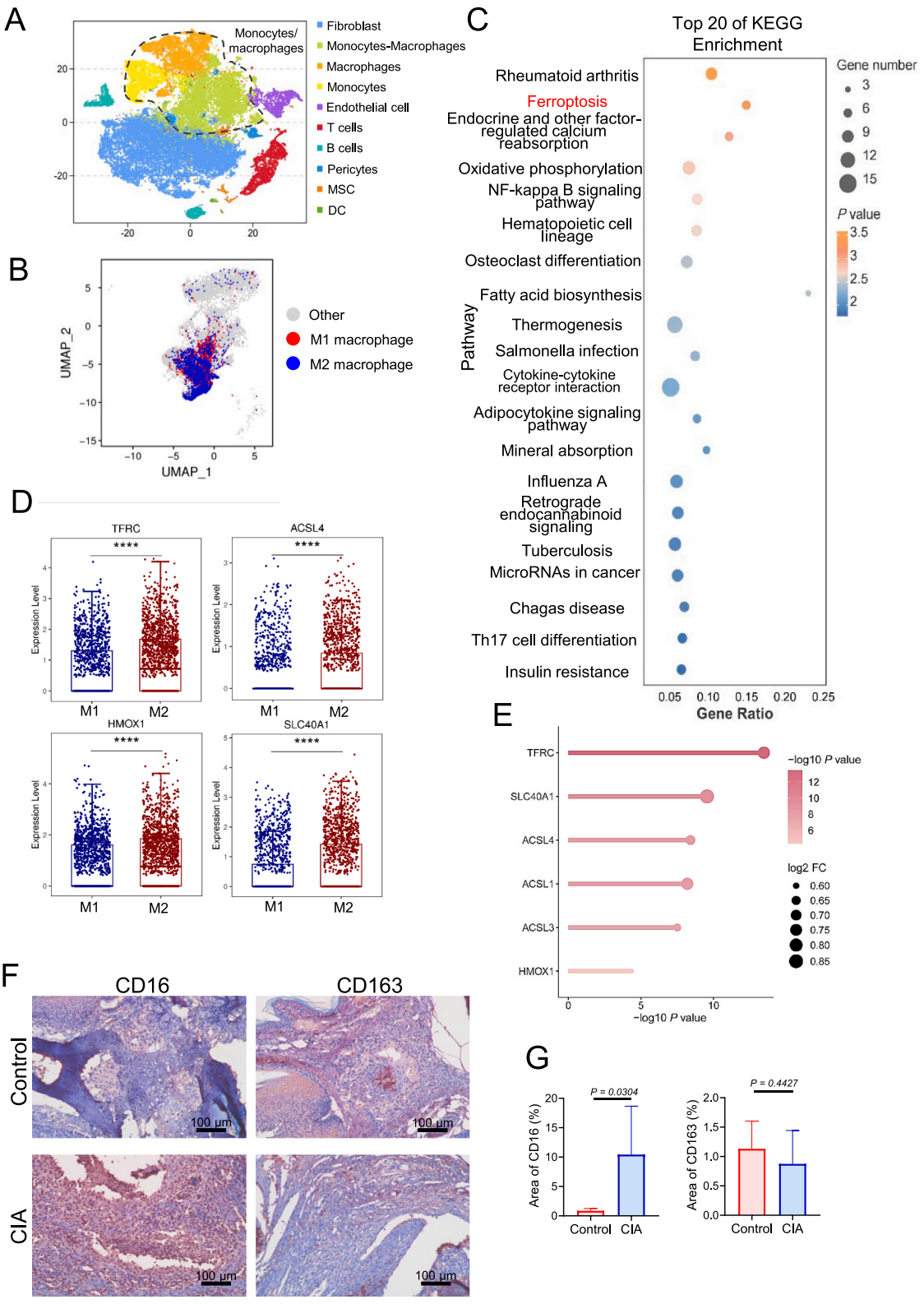

Fig. 2. $CD16^{low}CD64^{low}CD163^{high}MRC1^{high}$ macrophage subset may undergo ferroptosis in the progression of RA according to bioanalysis. **A** t-SNE plot displaying 56396 cells from the synovium of 5 RA patients separated into 10 major cell types, including fibroblast, macrophage-monocytes, monocytes, endothelial cells, T cells, B cells, pericytes, MSC and dendritic cell. **B** Predicted monocytes and macrophages subsets based on the expression levels of CD16, CD64, CD163 and MRC1 (M1 macrophages: $CD16^{high}CD64^{high}CD163^{low}MRC1^{low}$; M2 macrophages: $CD16^{low}CD64^{low}CD163^{high}MRC1^{high}$). **C** Enrichment analysis showing the 20 most significantly changed pathways in M2 macrophages, with red indicating pathways of interest. **D** Expression of four ferroptosis relevant genes: TFRC, ACSL4, HMOX1, and SLC40A1 in M1 macrophages and M2 macrophages subsets from RA subjects. **E** Lollipop plots of TFRC, SLC40A1, ACSL1, ACSL1, ACSL3, and HMOX1 expression in M2 subset compared with M1 subset from RA subjects. Immunohistochemical staining (**F**) and analysis (**G**) of CD16 and CD163 in the synovium of control and CIA mice (control group: n = 5; CIA group: n = 6). Data are presented as mean ± SD. (For interpretation of the references to colour in this figure legend, the reader is referred to the Web version of this article.)

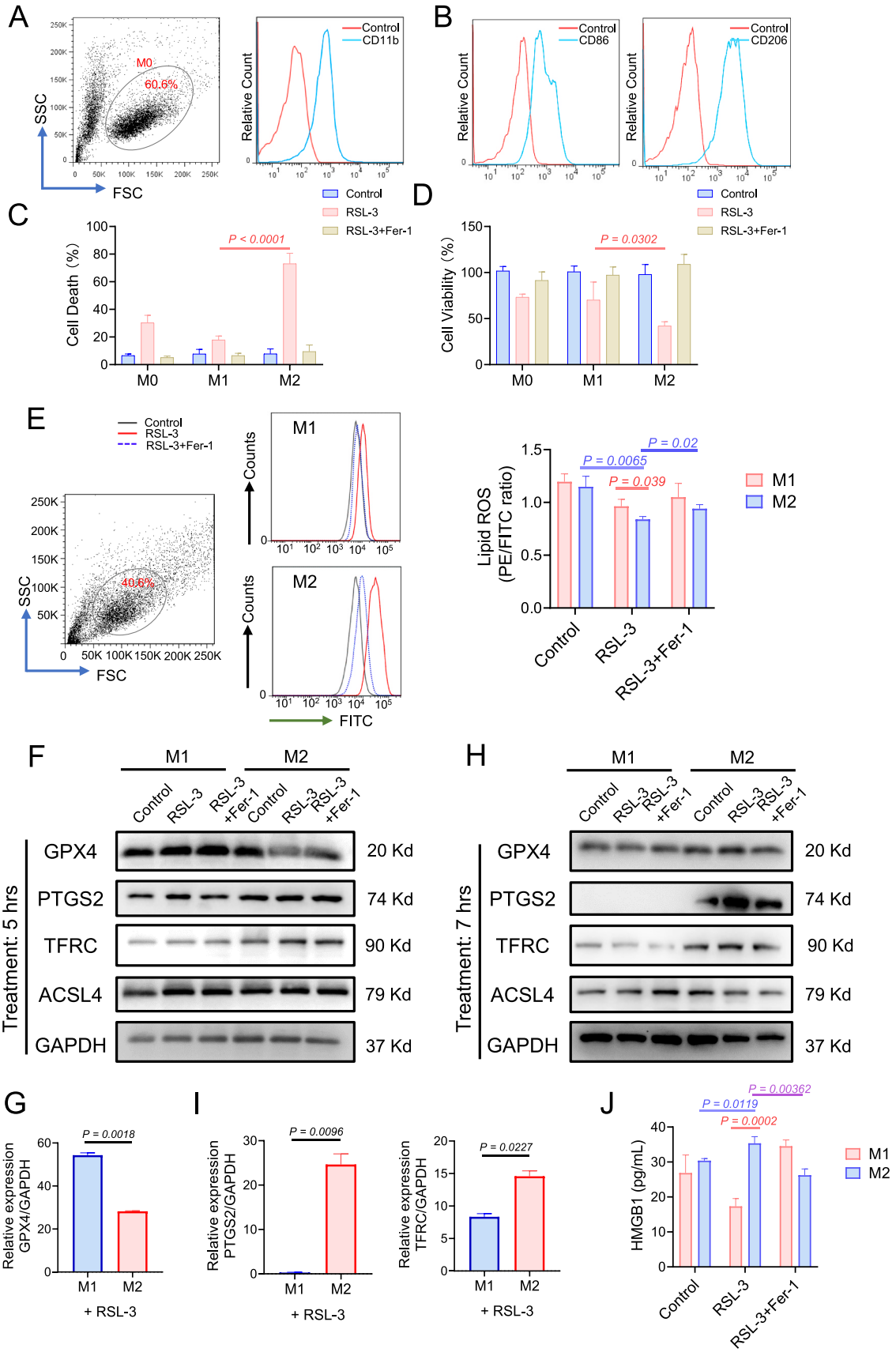

(caption on next page)

Fig. 3. M2 macrophages demonstrated greater sensitivity to ferroptosis compared to M1 macrophages polarized from THP-1 cells. **A** Gating strategy for differentially polarized THP-1 cells, with representative dot plots showing forward scatter (FSC) and side scatter (SSC) properties of M0 macrophages and measurement of CD11b protein expression via flow cytometry. **B** THP-1 cells were pretreated with 100 ng/mL of PMA for 72 h and incubated with LPS (100 ng/mL) and IFN-γ (20 ng/mL) or IL-4 (20 ng/mL) and IL-13 (20 ng/mL) for 48 h, with CD86 (M1) and CD206 (M2) expression levels measured via flow cytometry. **C** Cell death ratio were detected in M0, M1 and M2 macrophages derived from THP-1 cells with RSL-3 (0.75 μM, 5 h) treatment in the presence or absence of the ferroptosis inhibitor Fer-1 (1 μM). **D** Cell viability was assayed by measuring cellular ATP levels 5 h after RSL-3 treatment in the presence or absence of Fer-1. **E** Lipid ROS was measured by PE/FITC ratio by flow cytometry. **F** Ferroptosis related proteins GPX4, PTGS2, TFRC and ACSL4 were determined by western blotting in M1 and M2 macrophages polarized from THP-1 cells 5 h after RSL-3 treatment in the presence or absence of Fer-1, with quantification of GPX4 gray value normalized to GAPDH shown in **G**. **H** GPX4, PTGS2, TFRC and ACSL4 were determined by western blotting in M1 and M2 macrophages 7 h after RSL-3 treatment, with quantification of PTGS2 and TFRC gray value normalized to GAPDH shown in **I**. **J** Concentration of HMGB1 in the culture supernatant of M1 and M2 macrophages treated with RSL-3 (0.75 μM, 10 h) in the presence or absence of Fer-1. Values are shown as the means ± SD.

adeno-associated virus (AAV) overexpressing Gpx4 (AAV-DIO-Gpx4) or Gapdh (AAV-DIO-Gapdh) was injected into the articulus of myeloid-specific Lyz2-Cre line mice at 2, 4, and 7 days post the administration of collagen antibody (Fig. S6A), Moreover, the results indicated that the treatment with GPX4-overexpressing AAV mainly affected articular cartilage and alleviated joint inflammation and bone destruction (Fig. 5D and F). Furthermore, we found that the mitigation of arthritis symptoms caused by Lip-1 or AAV-DIO-Gpx4 was accompanied by a marked increase in the proportion of M2 macrophages (CD163) and a decrease in the proportion of M1 macrophages (CD16) in the synovium (Fig. 5G to H and Figs. S6D–E). Moreover, we isolated macrophages and found that the proportions of $CD206^{high}$ M2 macrophages in the synovium, spleen, and PBMCs were prominently greater in the Lip-1 administrated CIA group than in the CIA group, suggesting that Lip-1 pretreatment inhibits ferroptosis in M2 macrophages (Fig. 5I). mIHC analysis revealed that the levels of TLR4 and $p\text{-}STAT3^{S727}$ were significantly decreased in the hyperplastic synovium of arthritic mice treated with Lip-1 or AAV-DIO-Gpx4, whereas the expression level of GPX4 was increased in M2 macrophages (Fig. 6A–C, Fig. S6B to C and Fig. S6F to G). In addition, the expression levels of IL-1β and IL-6 were diminished in the synovium of the arthritic mice treated with Lip-1 or AAV-DIO-Gpx4, which is consistent with the morphological results of TRAP staining in the CIA and CAIA mouse models (Fig. 6D–G and Fig. S5).

These results confirmed that either Lip-1 pretreatment or AAV-DIO-Gpx4 treatment could protect M2 macrophages from ferroptosis and suppress the production of inflammatory cytokines by M1 macrophages, thereby mitigating osteoclast formation and the development of arthritis.

3. Discussion

As an incurable systemic autoimmune disease, RA progression leads to joint inflammation and destruction, which impacts the quality of life of patients [27]. The inflamed and hyperplastic synovial membrane of RA is characterized by the accumulation of innate and adaptive immune cells (e.g., macrophages, T cells, dendritic cells, B cells, and osteoclasts). Under conditions of RA inflammation, fibroblast-like synoviocytes (FLSs) in the synovium are also thought to have immune functions and show a special phenotype characterized by abnormal production of cytokines that perpetuate inflammation and overexpression of adhesion molecules and matrix metalloproteinases (MMPs) that contribute to cartilage destruction and joint damage [27]. In our previous study, we demonstrated that the hyperplastic rheumatoid synovium and synovial fluid of RA patients exhibit increased levels of lipid peroxidation and iron. TNF signaling promotes the biosynthesis of glutathione to protect fibroblasts from ferroptosis. The combination of a low-dose ferroptosis inducer, IKE, with the anti-TNF antagonist etanercept triggers fibroblast ferroptosis and leads to reduced cartilage and bone damage in a CIA mouse model after the onset of severe arthritis symptoms [15]. In addition to fibroblasts, macrophages are essential for the pathogenesis of RA. An early indicator of rheumatic disease is an increase in macrophages in the synovium sub-lining, and inflammatory lesions are frequently associated with high macrophage population [7]. Macrophages can differentiate into two different phenotypes, including inflammatory "M1" and anti-inflammatory "M2" macrophages, characterized by distinct functions. In the ferroptosis-promoting environment, the fate and function of different macrophage types attracted our attention. Both iron overload and ROS production reportedly contribute to M1 polarization [28]. Compared with M2 macrophages, M1 macrophages express more Hamp and FTH/FTL but less FPN and IRP1/2, indicating greater iron storage [28]. M1 macrophages also produce high levels of ROS and nitrogen species [29]. Further studies have shown that the generation of ROS is mainly due to the PTEN/AKT pathway, which activates NF-κB signaling [30]. M2 macrophages are more sensitive to ferroptosis than M1 macrophages because of the expression of iNOS, the enzyme responsible for NO production by M1 macrophages, which can inhibit lipid peroxidation [31]. Current therapeutic strategies for RA are aimed at targeting the unbalanced M1/M2 ratio. For example, macrophages can shift to an M2-like state in response to glucocorticoids, and a number of other DMARDs, including methotrexate and leflunomide and display similar mechanisms of action. Moreover, folic acid-modified silver nanoparticles have therapeutic effects on RA through M1-to-M2 macrophage repolarization [32]. A deeper understanding of the interplay between M1 or M2 macrophages and ferroptosis would assist in identifying novel therapeutic targets. Determining the precise role that M1 and M2 macrophages play in ferroptosis would assist in exploring novel targets for RA therapeutics.

It has been shown that iNOS-expressing M1 macrophages exhibit increased resistance to ferroptosis compared to M2 macrophages [31]. Consistent with these findings, we found that compared with M1 macrophages stimulated with RSL-3, M2 macrophages stimulated with RSL-3 exhibit increased cell death, lipid ROS levels, and iron levels and decreased cell viability. Furthermore, GPX4 is downregulated, while PTGS2 and TFRC are upregulated in M2 macrophages in the presence of RSL-3. The lethal accumulation of lipid peroxides is a cardinal feature of ferroptosis and involves antagonism between ferroptosis execution and ferroptosis defense systems in cells; ferroptosis occurs when ferroptosis-promoting cellular activities significantly override the antioxidant capabilities provided by ferroptosis defense systems [33–39]. We found that exposure of cells to ferroptosis inducers results in changes in ferroptosis-related molecules, including ferroptosis-promoting and ferroptosis-defending molecules, in a time-dependent manner. The expression level of GPX4 decreass significantly in M2 macrophages treated with RSL-3 for 5 h, whereas the GPX4 level seems to recover at 7 h. Cells stimulated with ferroptosis inducers frequently exhibit various stress defense mechanisms as well as other compensatory alterations. For example, exposure of cells to Fe^{2+} results in increased nuclear factor E2-related factor 2 (Nrf2) expression in a time- and concentration-dependent manner, which protects cells against ferroptosis [40–42]. Nrf2 is a transcription factor that regulates various antioxidant enzymes, including GPX4. The upregulation of GPX4 may be a protective mechanism under long-term stimulation with RSL-3. These data support the hypothesis that M2 macrophages are more vulnerable to ferroptosis in the microenvironment of the RA synovium with a high level of iron. A recent study also demonstrated that the different susceptibilities of macrophage subtypes to ferroptosis, caused by p62/SQSTM1-dependent autophagic degradation of GPX4, leads to subsequent immune cell imbalances in patients with RA [43]. These

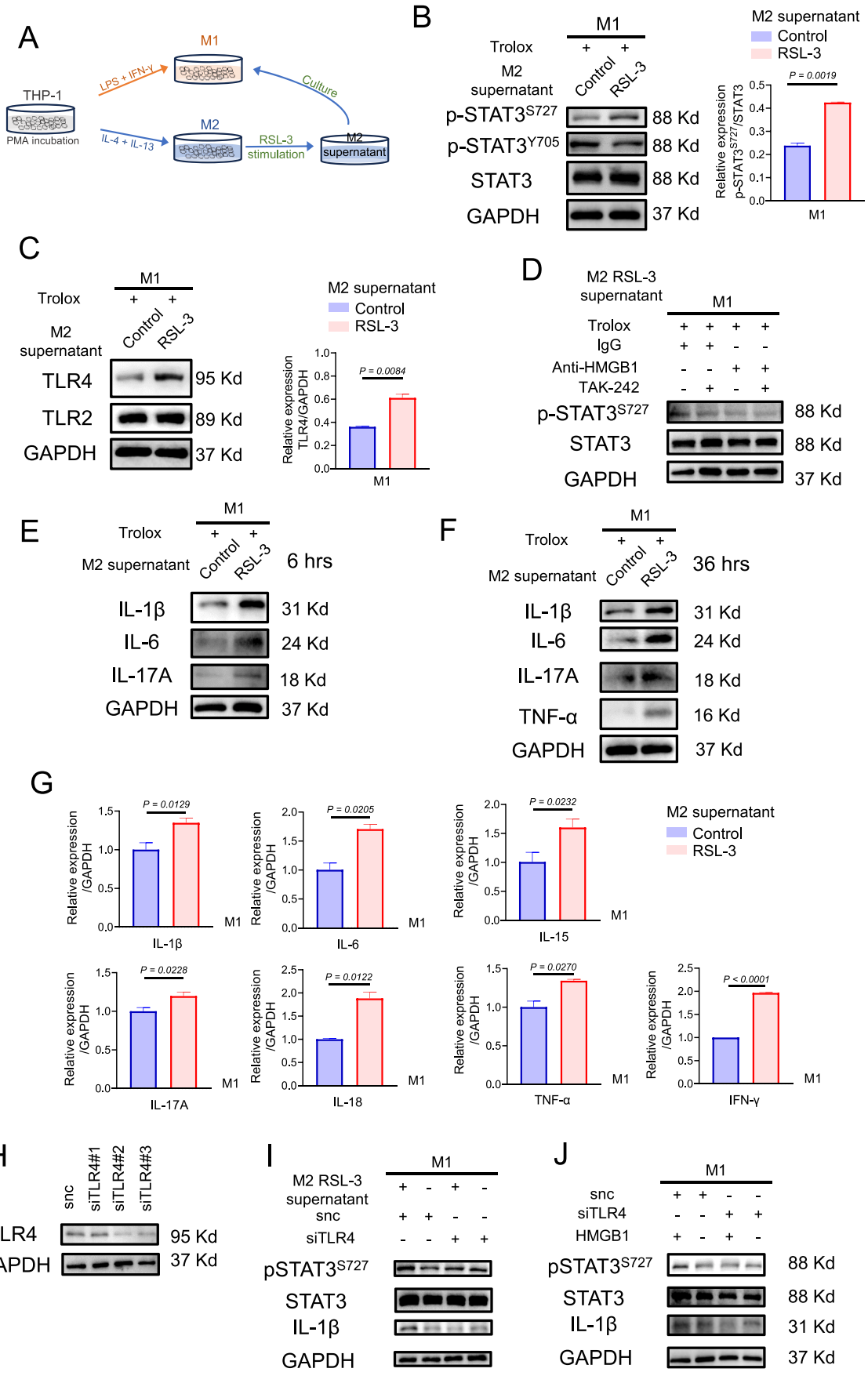

(caption on next page)

Fig. 4. HMGB1 secreted by RSL-3-stimulated M2 macrophages promoted the production of inflammatory cytokines in M1 macrophages. **A** Schematic diagram for constructing an indirect co-culture system of M2 and M1 macrophages. **B** Left, western blotting analysis of phospho-STAT3^{S727}, phospho-STAT3^{Y705} and STAT3 expression in M1 macrophages cultured for 6 h with M2 macrophage supernatant treated with RSL-3 (0.75 μM, 10 h). GAPDH was used as the loading control. Right, quantification of phospho-STAT3^{S727}/STAT gray value. **C** Left, western blotting of TLR4 and TLR2 expression in M1 macrophages cultured for 36 h with M2 macrophages supernatant treated with RSL-3 (0.75 μM, 10 h). Right, quantification of TLR4/GAPDH gray value. **D** Western blotting analysis of phospho-STAT3^{S727} and STAT3 expression in M1 macrophages cultured with the supernatant of RSL-3-treated M2 macrophages (RSL-3, 0.75 μM, 10 h) and exposure to HMGB1-specific blocking antibody in the presence or absence of the TLR4 inhibitor TAK-242 for 6 h. **E** Western blotting of IL-1β, IL-6, and IL-17A expression in M1 macrophages cultured for 6 h with M2 macrophages supernatant treated with RSL-3 (0.75 μM, 10 h). **F** Western blotting of IL-1β, IL-6, IL-17A and TNF-α expression in M1 macrophages cultured for 36 h with M2 macrophages supernatant treated with RSL-3 (0.75 μM, 10 h). **G** mRNA levels of inflammatory cytokines including IL-1β, IL-6, IL-17A, IL-15, IL-18, TNF-α and IFN-γ in M1 macrophages cultured with M2 macrophages supernatant treated with RSL-3. **H** Western blotting analysis of TLR4 expression in THP-1 cells transfected with scramble siRNA or one of three independent siRNAs targeting TLR4 (siTLR4#1, siTLR4#2, siTLR4#3). **I** Western blotting analysis of phospho-STAT3^{S727}, STAT3, and IL-1β expression in M1 macrophages transfected with scramble siRNA or siRNA targeting TLR4 and cultured for 36 h with M2 macrophages supernatant treated with RSL-3 (0.75 μM, 10 h). **J** Western blotting analysis of phospho-STAT3^{S727}, STAT3, and IL-1β expression in M1 macrophages transfected with scramble siRNA or siRNA targeting TLR4 and treated with HMGB1 protein (5 μg/mL) for 48 h. Values are shown as the means ± SD.

findings suggest that some molecules released by ferroptotic M2 macrophages may contribute to the exacerbation of joint inflammation, and this hypothesis was further supported by our research.

Pathogen-associated molecular pattern (PAMPS) and DAMPs, such as LPS, flagellin and dsRNA, can all potently stimulate macrophages to produce proinflammatory cytokines and exacerbate RA progression. Endogenous danger signals, or DAMPs, can initiate and sustain a noninfectious inflammatory response following cell death [44]. By identifying pathogens and DAMPs, TLRs, a major class of pattern recognition receptors (PRRs), mediate host defenses against infection and injury and are key determinants of inflammation [45]. TLR2 and TLR4 are highly expressed on CD16^{+} macrophages (a marker of M1 macrophages) in the synovium and peripheral blood mononuclear cells of RA patients. Increased production of IL-6, IL-8, and TNF was detected in RA synovial membrane cultures upon stimulation with TLR2 and TLR4 ligands [46]. HMGB1 is a DAMP that is released during ferroptosis [47]. The binding of HMGB1 to TLR4 leads to the activation of downstream signaling pathways through nuclear factor-κB (NF-κB) and the production of inflammatory mediators, including cytokines and chemokines [48–50]. Inhibition of the HMGB1/TLR4 pathway may effectively protect against LPS-induced ALI (acute lung injury). Notably, HMGB1/TLR4 may also mediate pathways independent of NF-κB. Our research revealed that HMGB1/TLR4 activates STAT3 via its phosphorylation at serine 727, which in turn increases the production of inflammatory cytokines by M1 macrophages. Additionally, we discovered that by interacting with TLR4 rather than TLR2, HMGB1 generated by ferroptotic M2 macrophages promotes the release of inflammatory cytokines from M1 macrophages. Our findings indicates that the distinct vulnerability of M1 and M2 macrophages to ferroptosis is an important reason for the exacerbation of synovial inflammation and the progression of RA. Due to the different vulnerability, the interaction between ferroptotic M2 macrophages and M1 macrophages escaping from ferroptosis further promotes the formation of an inflammatory microenvironment in the RA synovium.

Under inflammatory conditions, inflammatory stimuli such as IL-12 and ROS promote the polarization of macrophages toward the M1 phenotype, resulting in the release of cytokines such as IL-6 and IL-1 to affect osteoclast differentiation and formation [51–53]. In this study, we found that the expression levels of IL-1β and IL-6 in M1 macrophages are increased following treatment with the supernatant of ferroptotic M2 macrophages. Moreover, the levels of IL-1β and IL-6 are diminished in the synovium of the arthritic mice treated with Lip-1 or AAV-DIO-Gpx4. Consistently, the administration of the ferroptosis inhibitor Lip-1 started at the presymptomatic stages of CIA, and GPX4 overexpression in M2 macrophages at the onset of CAIA continuously prevent the formation of osteoclasts and the development of joint destruction. One of the mechanisms underlying their protective effects against RA is the prevention of M2 macrophage ferroptosis, which can rebalance the M1/M2 ratio, suppress osteoclasts-promoting cytokines secreted from M1 macrophages and maintain a normal immunological microenvironment. Interestingly, we previously reported that the administration of Lip-1 cannot suppress the development of inflammation or joint damage after the onset of severe arthritis symptoms [15]. The targeted regulation of fibroblasts or M2 macrophage ferroptosis may depend on the stage of RA, which is crucial for improving the therapeutic management of patients.

In conclusion, many diseases are linked to the process of cell death, and ferroptosis has recently been found to be crucial for the development of RA. M1/M2 macrophage imbalance caused by an increase in M1 macrophages or a decrease in M2 macrophages is common in inflammatory diseases [54]. Selectively targeting M2 macrophages to prevent ferroptotic cell death might be a novel therapeutic approach for these diseases.

4. Materials and methods

4.1. Establishment of collagen-induced arthritis (CIA) mouse model

Male DBA/1 mice (8–10 weeks old) were immunized with an emulsion of bovine type II collagen (CII) in complete Freund's adjuvant (CFA) to induce arthritis. A booster injection of CII in incomplete Freund's adjuvant (IFA) was administered 14 days post-immunization. Lip-1 was introduced into mice begining at day 7 after the first immunization (before inflammation onset). Vehicle for Lip-1: 5 % DMSO, 40 % PEG300, 5 % Tween80, 50 % ddH_2O. DBA/1 mice were observed every 2 days for signs of arthritis, based on paw swelling and arthritis scores. The level of inflammation for each paw was graded from 0 to 4 by the following scale: 0 = no damage; 1 = paw with detectable swelling in a single digit; 2 = paw with swelling in more than one digit; 3 = paw with swelling of all digits and instep; and 4 = severe swelling of the paw and ankle. The arthritic scores of four paws were summed. All procedures involving animals were approved by the Institutional Animal Care and Use Committee (IACUC) of the National Translational Science Center for Molecular Medicine, Fourth Military Medical University (Approval No. 2023-NTSCMM-ID005), and were conducted in accordance with national guidelines. DBA/1 mice were purchased from Cyagen Biosciences Co., Ltd. (Suzhou, China), and were maintained in a specific pathogen-free mouse facility (room temperature, 20 °C–22 °C; room humidity, 40 %–60 %, with free access to food and water) under a 12 h light/dark cycle.

4.2. Collagen antibody-induced arthritis (CAIA) mouse model and intra-articular delivery of GPX4 overexpressing adeno-associated virus (AAV)

C57BL/6J mice (8–10 weeks old, male) and Lyz2-Cre mice (8–10 weeks old, male, on a C57BL/6 background) were obtained from Cyagen Biosciences (Suzhou, China). The CAIA model was induced by intraperitoneal injection (i.p.) of a 5-clonal collagen antibody mixture (4 mg in PBS per mouse; day 0), followed by an intraperitoneal injection of lipopolysaccharide (LPS; 50 μg) on day 3. The control group received an equivalent volume of normal saline. On day 15, mice were euthanized under anesthesia. The criteria for joint swelling and arthritis index were

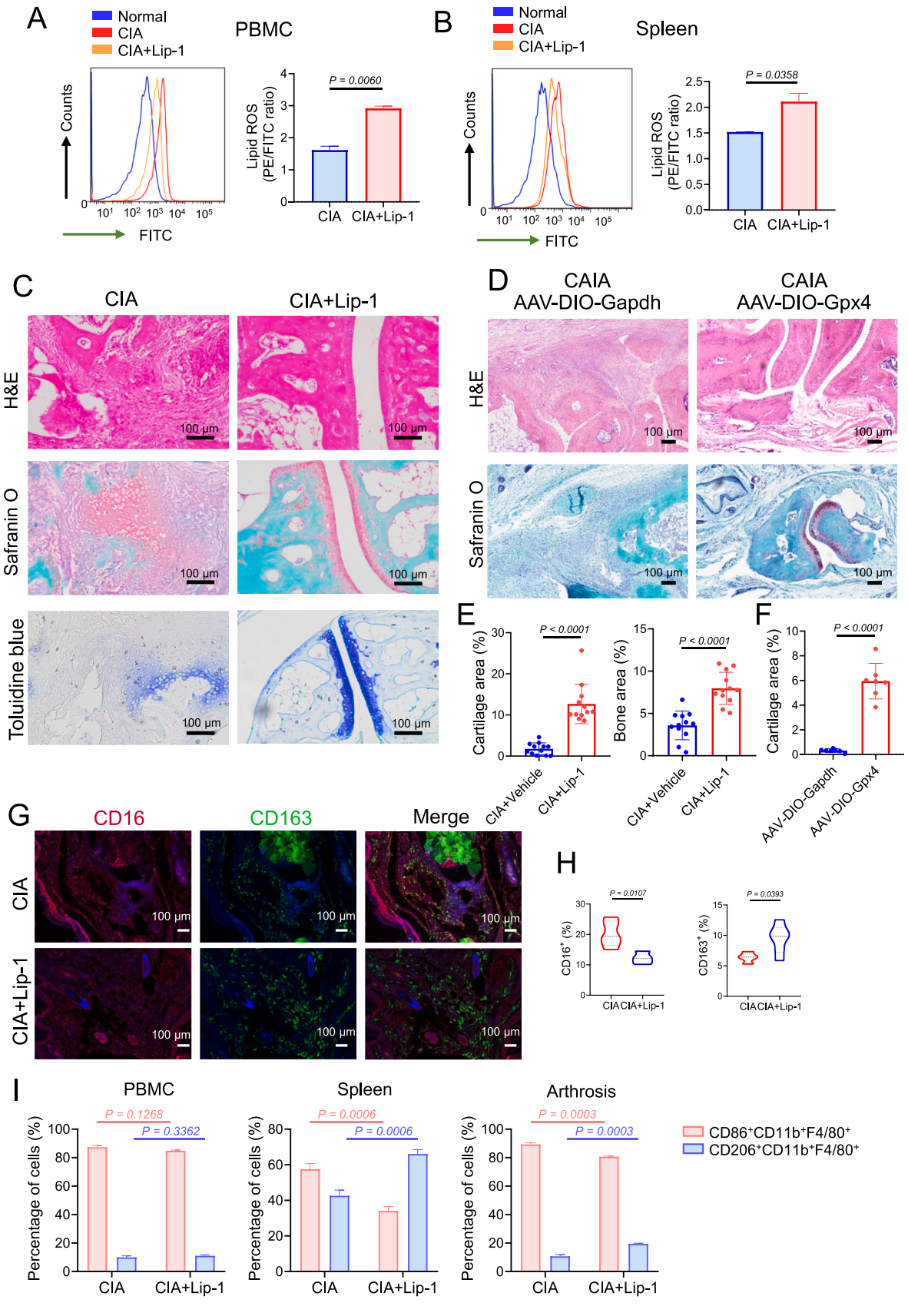

(caption on next page)

Fig. 5. GPX4 overexpression or ferroptosis inhibitor Lip-1 treatment started at the pre-symptomatic stages alleviated arthritis symptoms of CIA mice. **A** Flow cytometric analysis (left) of PBMC cells for FITC fluorescence and analysis of lipid peroxidation (right) from CIA mice with or without Lip-1 administration. **B** Flow cytometric analysis of spleen cells (left) for FITC fluorescence and analysis of lipid peroxidation (right). **C** Images of H&E, safranin O, and toluidine blue staining of representative joints in CIA mice with or without Lip-1 treatment on day 25 after treatment initiation. Scale bars, 100 μm. **D** Images of H&E, safranin O, and toluidine blue staining of representative joints in control and CAIA mice with or without AAV-DIO-Gpx4 treatment. Scale bars, 100 μm. **E** Quantification of the histomorphometric analysis of cartilage damage and bone erosion with n = 12 joints for both CIA and CIA + Lip-1 group. Data are presented as mean ± SD. **F** Quantification of the histo-morphometric analysis of CAIA mice cartilage damage, with n = 7 joints for both AAV-DIO-Gapdh and AAV-DIO-Gpx4 groups. Data are presented as mean ± SD. **G** Representative mIHC staining of inflamed joints of CIA mice treated with Lip-1 (10 mg/kg) and labeled with anti-CD16, anti-CD163 and DAPI. Similar results were observed from 8 joints tested for each group. Scale bars, 100 μm. **H** Quantification of the percentages of macrophage markers (M1: CD16; M2: CD163) in hyperplastic synovium. **I** The percentages of $CD86^+$ subset and $CD206^+$ subset in $CD11b^+F4/80^+$ macrophages from Lip-1 treated or untreated mice on day 39 was analyzed by flow cytometry, with n = 3 mice for each group. Data are presented as mean ± SD. (For interpretation of the references to colour in this figure legend, the reader is referred to the Web version of this article.)

consistent with those used in the CIA model. Disease-induced animals were selected and randomized into two treatment groups on day 2. Recombinant AAV overexpressing GPX4 (rAAV8-CMV-DIO-mCherry-2A-Gpx4-WPRE-hGH pA) and a control rAAV8-CMV-DIO-mCherry-2A-Gapdh-WPRE-hGH-pA were procured from BrainVTA (Wuhan, China). Intra-articular injections of AAV-DIO-Gpx4 or AAV-DIO-Gapdh (2×10^{12} copies) was administered to Lyz2-Cre CAIA mice at day 2, day 4, and day 7 post-induction. The NCBI gene IDs for Gapdh and Gpx4 are 14433 and 625249, respectively.

4.3. Single-cell RNA sequencing (RNA-seq)

Single-cell RNA-seq was conducted as previously described, with the data deposited in the NCBI Sequence Read Archive (SRA) under accession codes PRJNA725073. Differentially expressed genes analysis Expression value of each gene in given cluster were compared against the rest of cells using Wilcoxon rank sum test. Significant upregulated genes were identified using three criteria. First, genes had to be at least 1.28-fold overexpressed in the target cluster. Second, genes had to be expressed in more than 25 % of the cells belonging to the target cluster. Third, p value is less than 0.05.

4.4. Human specimen research

This study was approved by the Medical Ethics Committee of the First Affiliated Hospital (Xijing Hospital) of the Fourth Military Medical University (KY20192006–F-1). Informed written consent was obtained from all patients/patients' families prior to participation. The biopsies were obtained from key-hole arthroscopy (during arthroscopic cleansing of the knee). All RA (n = 5) and osteoarthritis (OA) (n = 5) patients fulfilled the clinical and radiographic criteria of the American College of Rheumatology. Detailed clinical characteristics were shown in Table S1.

4.5. Cell culture

THP-1 (TIB-202™) cells were purchased from the ATCC and cultured in RPMI-1640 medium (Thermo Scientific, 11875-093) supplemented with 10 % fetal bovine serum (Thermo Scientific, 10100-147-FBS), 1 % penicillin/streptomycin (Thermo scientific, 15240062), and 2 % L-glutamine at 37 °C in a 5 % CO_2 humidified atmosphere. Phorbol 12-myristate 13-acetate (PMA; 100 ng/mL) was employed to activate THP-1 cells. Following 72 h of PMA activation, THP-1 cells were differentiated into M1 macrophages by exposure to interferon-γ (IFN-γ; 20 ng/mL) and LPS (100 ng/mL). M2 macrophage polarization was induced by interleukin-4 (IL-4; 20 ng/mL) and interleukin-13 (IL-13; 20 ng/mL).

4.6. Flow cytometry

THP-1 cells were stained with antibodies recognizing surface markers: ITGAM/CD11b-FITC (Biolegend, 101206), CD206-APC (Biolegend, 321109), CD86-FITC (Biolegend, 374203). CIA mice macrophages from arthritic joints, spleen, and peripheral blood mononuclear cells (PBMC) were stained with ITGAM/CD11b-APC Cy7, F4/80-PerCP Cy5.5, CD86-PE Cy7, and CD206-APC. The Fluorescence Minus One (FMO) controls were used to determine the cut-off point between background fluorescence and positive populations. Analysis was performed using a BD Fortessa flow cytometer, with data processed via Flow Jo software.

4.7. Western blotting analysis

Protein samples prepared in SDS sample buffer were boiled and separated on 10 % SDS-polyacrylamide gel, and then the proteins were transferred to 0.45 μm polyvinylidene fluoride (PVDF) membranes. Membranes were incubated with primary antibodies, followed by HRP-conjugated secondary antibodies. Detection was achieved using an enhanced chemiluminescence substrate, as per the manufacturer's instructions. The antibodies used are listed in Table S2.

4.8. RNA extraction and quantitative real-time PCR

Total RNA of M1 macrophages cultured with M2 macrophages supernatant after RSL-3 treatment was extracted using a Total RNA Kit (D6934-01, Omega Biotek, Norcross, American) according to the manufacturer's instructions. RNA purity and concentration were analyzed using a Nanodrop 2000 (Thermo Fisher Scientific). cDNA was synthesized using Superscript First Strand Synthesis Kit (Invitrogen). Next, qRT-PCR was performed using a SYBR Green PCR kit (TaKaRa, Otsu, Japan) on the MxPro system to determine the expression levels of the genes of interest. The primers are listed in Table S3.

4.9. Immunohistochemistry assay

Tissues were fixed in 10 % neutral buffered formalin for 24 h and decalcified with 15% EDTA for 3-4 weeks. Following decalcification, the tissues were dehydrated through a graded ethanol series, embedded in paraffin, and sectioned at 3 μm onto polylysine-coated slides. Slides were rehydrated with decreasing percentage of ethanol solutions and subjected to stains. Immunohistochemical staining was performed using a streptavidin–peroxidase kit (ZSGB-Bio, China). The primary antibodies targeted the following proteins: RANKL (Abcam, ab216484), M-CSF (HuaBio, ET1609-1), CD16 (Abcam, ab203883), CD163 (HuaBio, ER1804-03), with a standard avidin-biotin HRP detection system according to the instructions of the manufacturer (anti-mouse/rabbit HRP-DAB Cell & Tissue Staining Kit, R&D Systems Minneapolis, MN). Tissue sections were counterstained with hematoxylin, dehydrated, and mounted. Quantitative analysis was conducted using Image-Pro Plus software, Version 6.0.

4.10. Multiplex immunohistochemistry (mIHC) staining

mIHC staining was performed using 3-μm-thick sections of formalin-fixed and paraffin-embedded tissues. Briefly, slides were deparaffinized in xylene and hydrated in ethanol at gradient concentrations. After trypsin induced antigen retrieval, the samples were blocked with 5 %

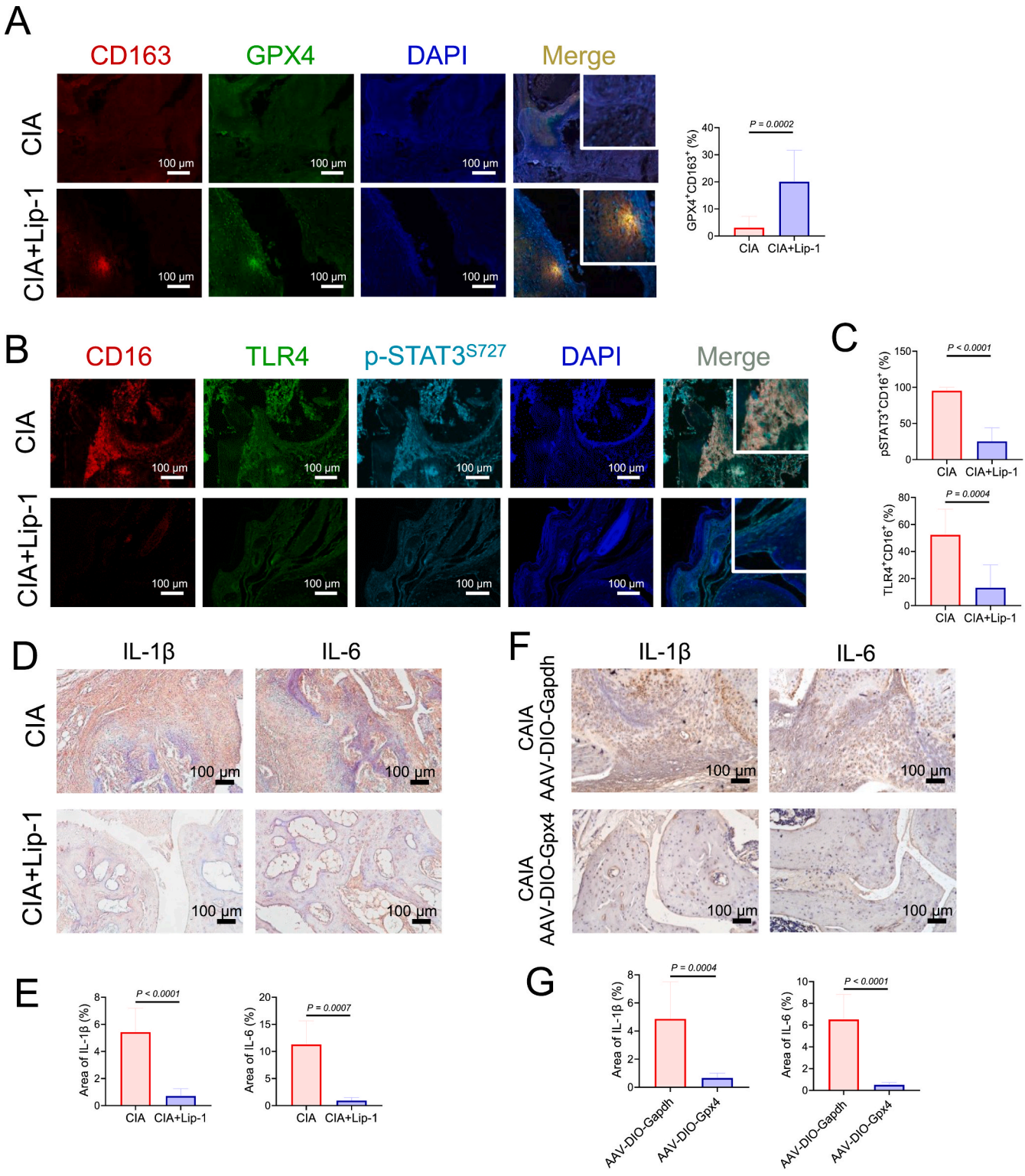

Fig. 6. GPX4 overexpression or ferroptosis inhibitor Lip-1 treatment ameliorate arthritis progression by protecting M2 macrophages from ferroptosis and decreasing the levels of IL-1β and IL-6. **A** Representative mIHC staining of inflamed joints labeled with anti-CD163, anti-GPX4 and DAPI. Scale bars, 100 μm. **B** Representative fluorescent mIHC staining of joints labeled with anti-CD16, anti-TLR4, anti-phophoSTAT3^{S727} and DAPI. Scale bars, 100 μm. **C** Quantification of the percentages of TLR4^{+} CD16^{+} and p-STAT3^{+}CD16^{+} cells by calculating the immunofluorescence using inForm software cell analysis. **D** Immunohistochemical staining of IL-1β and IL-6 from Lip-1 treated or untreated mice on day 39 (n = 8). Scale bars, 100 μm. **E** Quantification of the histomorphometric analysis of the expression of IL-1β and IL-6 in **D**. **F** Immunohistochemical staining of IL-1β and IL-6 from AAV-DIO-Gapdh or AAV-DIO-Gpx4 treatment treated mice (n = 3). Scale bars, 100 μm. **G** Quantification of the histomorphometric analysis of the expression of IL-1β and IL-6 in **F**. Data are presented as mean ± SD.

goat serum-PBS, and stained with primary antibodies. Nuclei were stained with DAPI. A TSA-indirect kit was used according to the manufacturer's instructions (PerkinElmer). Image analysis was performed using inForm software, Version 2.4.

4.11. Assessment of cell death, viability, and lipid peroxidation

Cell death was evaluated using SYTOX Green staining, followed by microscopy or flow cytometry. Cell viability was determined using the CellTiter-Glo™ Luminescent Cell Viability Assay (Promega, G7571) according to the manufacturer's instructions, with ATP levels normalized to control cells. For lipid peroxidation, cells were incubated with a Lipid Peroxidation Sensor (Abcam, ab243377) in a humidified chamber at 37 °C with 5 % CO_2 for 30 min, and changes in fluorescence from PE to FITC were measured using flow cytometry, allowing for ratio-metric assessment of lipid peroxidation levels. The decreasing PE/FITC ratio means increasing lipid peroxidation.

4.12. Measurement of ROS and cellular iron accumulation

Experiments were performed according to the manufacturer's protocol. Cells were incubated in a humidified chamber at 37 °C with 5 % CO_2 for 30 min with DCFH-DA in cell culture medium. After incubation, cells were washed and examined by flow cytometry within 2 h of staining. Cells were washed with PBS twice and stained with 1 μM of FerroOrange (Fe^{2+} indicator) for 30 min in 37 °C. After staining, cells were monitored by fluorescence intensity.

4.13. RNA interference and transfection

Sequences of three pairs of TLR4 siRNAs (Tsingke Biotechnology Co., Ltd., Beijing, China) are listed in Table S4. Transfection of M1 macrophages derived from THP-1 cells was performed using Hi-Perfect transfection reagent. The siRNA-transfection complex was formed and applied to cells, with a final concentration of 100 nM TLR4 siRNA. Successful transfection was confirmed by assessing protein expression changes after 48 h.

4.14. Tartrate-resistant acid phosphatase (TRAP) staining

TRAP activity is regarded as an important marker of osteoclasts. TRAP staining was performed using 3-μm-thick sections of formalin-fixed and paraffin-embedded tissues. It was carried out in accordance with the manufacturer's instruction (Solarbio Science & Technology Co., Ltd, Beijing, China).

4.15. Statistical analysis

Unless otherwise stated, data are presented as mean ± SD. A two-tailed Student's t-test or one-way ANOVA was used for analysis of differences. Statistical analysis was performed using GraphPad Prism 7.0 (GraphPad Prism Software, CA, USA). Differences considered to be significant when $p < 0.05$.

Funding

This study was supported by the National Natural Science Foundation of China 82270078 (to J.W.), Top Team in Strategy of Sanqin Talent Special Support Program of Shaanxi Province (to J.W.), Youth Innovation Team of Shaanxi Province (to J.W.) and Science and Technology Project of Shaanxi Province 2023-CX-PT-18 (to Z.F.).

CRediT authorship contribution statement

Zhuan Feng: Writing – original draft, Project administration, Methodology, Investigation, Data curation. **Feiyang Meng:** Investigation. **Fei Huo:** Methodology. **Yumeng Zhu:** Investigation. **Yifei Qin:** Methodology. **Yu Gui:** Methodology. **Hai Zhang:** Investigation, Formal analysis. **Peng Lin:** Investigation, Formal analysis. **Qian He:** Software, Investigation. **Yong Li:** Supervision. **Jiejie Geng:** Methodology, Investigation. **Jiao Wu:** Writing – review & editing, Writing – original draft, Methodology, Investigation, Data curation.

Declaration of competing interest

The authors have no conflict of interest relevant to this study to declare.

Data availability

Data will be made available on request.

Appendix A. Supplementary data

Supplementary data to this article can be found online at https://doi.org/10.1016/j.redox.2024.103255.

References

[1] K. Chauhan, J.S. Jandu, L.H. Brent, M.A. Al-Dhahir, in: StatPearls, 2024.
[2] G. Arango Duque, A. Descoteaux, Macrophage cytokines: involvement in immunity and infectious diseases, Front. Immunol. 5 (2014) 491, https://doi.org/10.3389/fimmu.2014.00491.
[3] A. Shapouri-Moghaddam, et al., Macrophage plasticity, polarization, and function in health and disease, J. Cell. Physiol. 233 (2018) 6425–6440, https://doi.org/10.1002/jcp.26429.
[4] M. Cutolo, R. Campitiello, E. Gotelli, S. Soldano, The role of M1/M2 macrophage polarization in rheumatoid arthritis synovitis, Front. Immunol. 13 (2022) 867260, https://doi.org/10.3389/fimmu.2022.867260.
[5] G. Zizzo, B.A. Hilliard, M. Monestier, P.L. Cohen, Efficient clearance of early apoptotic cells by human macrophages requires M2c polarization and MerTK induction, J. Immunol. 189 (2012) 3508–3520, https://doi.org/10.4049/jimmunol.1200662.
[6] X. Yang, Y. Chang, W. Wei, Emerging role of targeting macrophages in rheumatoid arthritis: focus on polarization, metabolism and apoptosis, Cell Prolif. 53 (2020) e12854, https://doi.org/10.1111/cpr.12854.
[7] I.A. Udalova, A. Mantovani, M. Feldmann, Macrophage heterogeneity in the context of rheumatoid arthritis, Nat. Rev. Rheumatol. 12 (2016) 472–485, https://doi.org/10.1038/nrrheum.2016.91.
[8] M.H. Abdelaziz, et al., Alternatively activated macrophages; a double-edged sword in allergic asthma, J. Transl. Med. 18 (2020) 58, https://doi.org/10.1186/s12967-020-02251-w.
[9] A. Saradna, D.C. Do, S. Kumar, Q.L. Fu, P. Gao, Macrophage polarization and allergic asthma, Transl. Res. 191 (2018) 1–14, https://doi.org/10.1016/j.trsl.2017.09.002.
[10] W. Zhu, et al., Anti-citrullinated protein antibodies induce macrophage subset disequilibrium in RA patients, Inflammation 38 (2015) 2067–2075, https://doi.org/10.1007/s10753-015-0188-z.
[11] S. Tardito, et al., Macrophage M1/M2 polarization and rheumatoid arthritis: a systematic review, Autoimmun. Rev. 18 (2019) 102397, https://doi.org/10.1016/j.autrev.2019.102397.
[12] S. Fukui, et al., M1 and M2 monocytes in rheumatoid arthritis: a contribution of imbalance of M1/M2 monocytes to osteoclastogenesis, Front. Immunol. 8 (2017) 1958, https://doi.org/10.3389/fimmu.2017.01958.
[13] W. Luczaj, et al., The onset of lipid peroxidation in rheumatoid arthritis: consequences and monitoring, Free Radic. Res. 50 (2016) 304–313, https://doi.org/10.3109/10715762.2015.1112901.
[14] G. Kaur, A. Sharma, A. Bhatnagar, Role of oxidative stress in pathophysiology of rheumatoid arthritis: insights into NRF2-KEAP1 signalling, Autoimmunity 54 (2021) 385–397, https://doi.org/10.1080/08916934.2021.1963959.
[15] J. Wu, et al., TNF antagonist sensitizes synovial fibroblasts to ferroptotic cell death in collagen-induced arthritis mouse models, Nat. Commun. 13 (2022) 676, https://doi.org/10.1038/s41467-021-27948-4.
[16] B. Raynaud-Messina, C. Verollet, I. Maridonneau-Parini, The osteoclast, a target cell for microorganisms, Bone 127 (2019) 315–323, https://doi.org/10.1016/j.bone.2019.06.023.
[17] T. Hasegawa, et al., Identification of a novel arthritis-associated osteoclast precursor macrophage regulated by FoxM1, Nat. Immunol. 20 (2019) 1631–1643, https://doi.org/10.1038/s41590-019-0526-7.
[18] S. Umar, et al., CCL25 and CCR9 is a unique pathway that potentiates pannus formation by remodeling RA macrophages into mature osteoclasts, Eur. J. Immunol. 51 (2021) 903–914, https://doi.org/10.1002/eji.202048681.
[19] Z. Zhuang, et al., Induction of M2 macrophages prevents bone loss in murine periodontitis models, J. Dent. Res. 98 (2019) 200–208, https://doi.org/10.1177/0022034518805984.

[20] I.E. Adamopoulos, E.D. Mellins, Alternative pathways of osteoclastogenesis in inflammatory arthritis, Nat. Rev. Rheumatol. 11 (2015) 189–194, https://doi.org/10.1038/nrrheum.2014.198.
[21] K. Hu, Z. Shang, X. Yang, Y. Zhang, L. Cao, Macrophage polarization and the regulation of bone immunity in bone homeostasis, J. Inflamm. Res. 16 (2023) 3563–3580, https://doi.org/10.2147/JIR.S423819.
[22] Z.C. Li, et al., Correlation of synovial fluid HMGB-1 levels with radiographic severity of knee osteoarthritis, Clin. Invest. Med. 34 (2011) E298, https://doi.org/10.25011/cim.v34i5.15673.
[23] P. Oktayoglu, et al., Elevated serum levels of high mobility group box protein 1 (HMGB1) in patients with ankylosing spondylitis and its association with disease activity and quality of life, Rheumatol. Int. 33 (2013) 1327–1331, https://doi.org/10.1007/s00296-012-2578-y.
[24] I. Kaur, et al., Exploring the therapeutic promise of targeting HMGB1 in rheumatoid arthritis, Life Sci. 258 (2020) 118164, https://doi.org/10.1016/j.lfs.2020.118164.
[25] U. Andersson, H. Erlandsson-Harris, HMGB1 is a potent trigger of arthritis, J. Intern. Med. 255 (2004) 344–350, https://doi.org/10.1111/j.1365-2796.2003.01303.x.
[26] M. Cutolo, et al., CTLA4-Ig treatment induces M1-M2 shift in cultured monocyte-derived macrophages from healthy subjects and rheumatoid arthritis patients, Arthritis Res. Ther. 23 (2021) 306, https://doi.org/10.1186/s13075-021-02691-9.
[27] Q. Ding, et al., Signaling pathways in rheumatoid arthritis: implications for targeted therapy, Signal Transduct. Targeted Ther. 8 (2023) 68, https://doi.org/10.1038/s41392-023-01331-9.
[28] Y. Yang, et al., Interaction between macrophages and ferroptosis, Cell Death Dis. 13 (2022) 355, https://doi.org/10.1038/s41419-022-04775-z.
[29] S.J. Koo, N.J. Garg, Metabolic programming of macrophage functions and pathogens control, Redox Biol. 24 (2019) 101198, https://doi.org/10.1016/j.redox.2019.101198.
[30] F. Huang, et al., miR-148a-3p mediates notch signaling to promote the differentiation and M1 activation of macrophages, Front. Immunol. 8 (2017) 1327, https://doi.org/10.3389/fimmu.2017.01327.
[31] A.A. Kapralov, et al., Redox lipid reprogramming commands susceptibility of macrophages and microglia to ferroptotic death, Nat. Chem. Biol. 16 (2020) 278–290, https://doi.org/10.1038/s41589-019-0462-8.
[32] Y. Yang, et al., Targeted silver nanoparticles for rheumatoid arthritis therapy via macrophage apoptosis and Re-polarization, Biomaterials 264 (2021) 120390, https://doi.org/10.1016/j.biomaterials.2020.120390.
[33] W.S. Yang, et al., Regulation of ferroptotic cancer cell death by GPX4, Cell 156 (2014) 317–331, https://doi.org/10.1016/j.cell.2013.12.010.
[34] K. Bersuker, et al., The CoQ oxidoreductase FSP1 acts parallel to GPX4 to inhibit ferroptosis, Nature 575 (2019) 688–692, https://doi.org/10.1038/s41586-019-1705-2.
[35] S. Doll, et al., FSP1 is a glutathione-independent ferroptosis suppressor, Nature 575 (2019) 693–698, https://doi.org/10.1038/s41586-019-1707-0.
[36] M. Soula, et al., Metabolic determinants of cancer cell sensitivity to canonical ferroptosis inducers, Nat. Chem. Biol. 16 (2020) 1351–1360, https://doi.org/10.1038/s41589-020-0613-y.
[37] X. Jiang, B.R. Stockwell, M. Conrad, Ferroptosis: mechanisms, biology and role in disease, Nat. Rev. Mol. Cell Biol. 22 (2021) 266–282, https://doi.org/10.1038/s41580-020-00324-8.
[38] C. Mao, et al., DHODH-mediated ferroptosis defence is a targetable vulnerability in cancer, Nature 593 (2021) 586–590, https://doi.org/10.1038/s41586-021-03539-7.
[39] G. Lei, L. Zhuang, B. Gan, Targeting ferroptosis as a vulnerability in cancer, Nat. Rev. Cancer 22 (2022) 381–396, https://doi.org/10.1038/s41568-022-00459-0.
[40] W.Y. Cheung, et al., Pannexin-1 and P2X7-receptor are required for apoptotic osteocytes in fatigued bone to trigger RANKL production in neighboring bystander osteocytes, J. Bone Miner. Res. 31 (2016) 890–899, https://doi.org/10.1002/jbmr.2740.
[41] D. Shin, E.H. Kim, J. Lee, J.L. Roh, Nrf2 inhibition reverses resistance to GPX4 inhibitor-induced ferroptosis in head and neck cancer, Free Radic. Biol. Med. 129 (2018) 454–462, https://doi.org/10.1016/j.freeradbiomed.2018.10.426.
[42] X. Jin, et al., Ferroptosis: emerging mechanisms, biological function, and therapeutic potential in cancer and inflammation, Cell Death Dis. 10 (2024) 45, https://doi.org/10.1038/s41420-024-01825-7.
[43] Y. Liu, et al., Heterogeneous ferroptosis susceptibility of macrophages caused by focal iron overload exacerbates rheumatoid arthritis, Redox Biol. 69 (2024) 103008, https://doi.org/10.1016/j.redox.2023.103008.
[44] J.S. Roh, D.H. Sohn, Damage-associated molecular patterns in inflammatory diseases, Immune Netw 18 (2018) e27, https://doi.org/10.4110/in.2018.18.e27.
[45] J. Kaur, H. Singh, S. Naqvi, Intracellular DAMPs in neurodegeneration and their role in clinical therapeutics, Mol. Neurobiol. 60 (2023) 3600–3616, https://doi.org/10.1007/s12035-023-03289-9.
[46] M. Iwahashi, et al., Expression of Toll-like receptor 2 on CD16+ blood monocytes and synovial tissue macrophages in rheumatoid arthritis, Arthritis Rheum. 50 (2004) 1457–1467, https://doi.org/10.1002/art.20219.
[47] Q. Wen, J. Liu, R. Kang, B. Zhou, D. Tang, The release and activity of HMGB1 in ferroptosis, Biochem. Biophys. Res. Commun. 510 (2019) 278–283, https://doi.org/10.1016/j.bbrc.2019.01.090.
[48] O.O. Ojo, M.H. Ryu, A. Jha, H. Unruh, A.J. Halayko, High-mobility group box 1 promotes extracellular matrix synthesis and wound repair in human bronchial epithelial cells, Am. J. Physiol. Lung Cell Mol. Physiol. 309 (2015) L1354–L1366, https://doi.org/10.1152/ajplung.00054.2015.
[49] D. Tang, R. Kang, H.J. Zeh, M.T. Lotze, The multifunctional protein HMGB1: 50 years of discovery, Nat. Rev. Immunol. 23 (2023) 824–841, https://doi.org/10.1038/s41577-023-00894-6.
[50] H. Yang, et al., A critical cysteine is required for HMGB1 binding to Toll-like receptor 4 and activation of macrophage cytokine release, Proc. Natl. Acad. Sci. U. S. A. 107 (2010) 11942–11947, https://doi.org/10.1073/pnas.1003893107.
[51] J. Jules, et al., Molecular basis of requirement of receptor activator of nuclear factor kappaB signaling for interleukin 1-mediated osteoclastogenesis, J. Biol. Chem. 287 (2012) 15728–15738, https://doi.org/10.1074/jbc.M111.296228.
[52] Y.C. Liu, X.B. Zou, Y.F. Chai, Y.M. Yao, Macrophage polarization in inflammatory diseases, Int. J. Biol. Sci. 10 (2014) 520–529, https://doi.org/10.7150/ijbs.8879.
[53] Y. Sun, et al., Macrophage-osteoclast associations: origin, polarization, and subgroups, Front. Immunol. 12 (2021) 778078, https://doi.org/10.3389/fimmu.2021.778078.
[54] M. Luo, F. Zhao, H. Cheng, M. Su, Y. Wang, Macrophage polarization: an important role in inflammatory diseases, Front. Immunol. 15 (2024) 1352946, https://doi.org/10.3389/fimmu.2024.1352946.